Fullerene Dications and Tricications as Initiators in the Gas-Phase "Ball-and-Chain" Polymerization of Allene and Propyne: Observation of a Remarkable Periodicity in Chain Growth with Allene

Vladimir Baranov,[†] Jinru Wang,[§] Gholamreza Javahery,[†] Simon Petrie,[‡] Alan C. Hopkinson, and Diethard K. Bohme*

Contribution from the Department of Chemistry and Centre for Research in Earth and Space Science, York Universiy, North York, Ontario, Canada M3J 1P3

Received April 25, 1996[⊗]

Abstract: The chemistry initiated by C_{60}^{x+} (with $x = 1$, 2, and 3) in allene and propyne has been tracked in the gas phase. Reaction rate coefficients and product distributions were measured with the Selected-Ion Flow Tube (SIFT) technique operating at 294 ± 3 K and at a helium buffer-gas pressure of 0.35 ± 0.01 Torr. $C_{60}^{\bullet+}$ does not react with allene and propyne under SIFT conditions, but multiple addition was observed with C_{60}^{2+}. Multiple addition was also observed in the reaction of propyne with C_{60}^{3+}, but allene reacted only by electron transfer with this cation. Up to 16 molecules of allene were observed to add to C_{60}^{2+} with a remarkable periodicity in reactivity: even-numbered adducts react approximately 10 times faster than odd-numbered adducts. Multi-collision induced dissociation (CID) experiments demonstrated that the observed multiple-adduct ions have a "ball-and-chain" structure. Mechanisms are proposed for the sequential addition reactions and for the formation of $C_6H_7^+$ and $C_9H_{12}^+$ which was seen to compete with multiple addition in the reactions of allene with C_{60}^{2+} and of propyne with C_{60}^{3+}. The multiple-addition reactions are proposed to occur by chain propagation. The periodicity in the rates of the reactions of allene with $C_{60}(\text{allene})_n^{2+}$ is attributed to differences in charge distribution and stability associated with an alternating formation of acyclic and cyclic structures.

Introduction

Two of the many remarkable attributes of Buckminsterfullerene, C_{60}, are the stability of its multiply-charged cations against Coulombic explosion and the high chemical reactivity of these cations in the gas phase. Up to seven electrons now have been removed from C_{60} in the gas phase[1] and already more than 100 gas-phase addition reactions which lead to the chemical derivatization of C_{60}^+, C_{60}^{2+}, and C_{60}^{3+} have been observed in our laboratory.[2] Furthermore, we have found that the chemistry initiated by multiply-charged fullerene cations often leads to *multiple additions*. For example, we have previously observed sequential addition of up to six molecules for the reactions of C_{60}^{2+} and C_{70}^{2+} with 1,3-butadiene,[3] of C_{60}^{2+} with ethylene oxide,[4] of C_{60}^{2+} with 1-butene,[5] of C_{58}^{3+} and C_{60}^{3+} with acetylene,[6] and of C_{60}^{3+} with ethylene.[6] Not surprisingly, the number of molecules observed to add and the kinetics of the sequential addition reactions are dependent on the nature of the added molecule. We have proposed that these multiple-addition reactions proceed via a "ball-and-chain" mechanism as shown in reaction 1 rather than through the formation of a "fuzzy ball" according to reaction 2. The first direct evidence for the "ball-and-chain" mechanism has come from very recent CID experiments in our laboratory with multiply-derivatized $C_{60}(1\text{-butene})_n^{2+}$.[5]

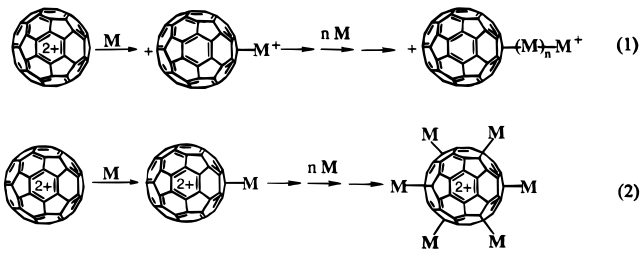

So far, we have found that addition reactions with singly-charged C_{60}^+ are rare and that this cation does not often induce multiple addition with common organic monomers.[2] This is in contrast to the cation-induced polymerization of organic monomers which has been observed with bare metal and other singly-charged cations in the gas phase. For example, polymerization has been observed with ethylene[7] and isobutylene[8] induced by Ti^+, with isobutylene induced by Zn^+,[9] with acetylene,[10]

[†] Present Address: SCIEX MDS Health Group, 71 Four Valley Drive, Concord, Ontario, Canada L4K 4V8.

[§] Department of Chemistry, University of British Columbia, 2036 Main Mall, Vancouver, B.C., Canada V6T 1Z1.

[‡] School of Chemistry, University College, University of New South Wales, A.D.F.A., Canberra, A.C.T. 2600, Australia.

[⊗] Abstract published in *Advance ACS Abstracts,* February 1, 1997.

(1) Scheier, P.; Märk, T. D. *Phys. Rev. Lett.* **1994**, *75*, 54.

(2) For a review see: Bohme, D. K. In *Recent Advances in the Chemistry and Physics of Fullerenes and Related Materials*; Ruoff, R. S., Kadish, K. M., Eds.; Electrochemical Society Proceedings 95−10, 1465; Electrochemical Society, Inc.: Pennington, NJ, 1995.

(3) Wang, J.; Javahery, G.; Petrie, S.; Bohme, D. K. *J. Am. Chem. Soc.* **1992**, *114*, 9665.

(4) Wang, J.; Javahery, G.; Petrie, S.; Hopkinson, A. C.; Bohme, D. K. *Angew. Chem., Int. Ed. Engl.* **1994**, *33(2)*, 206.

(5) Wang, J.; Baranov, V.; Bohme, D. K. *J. Am. Soc. Mass Spectrom.* **1996**, 7, 261.

(6) Wang, J.; Javahery, G.; Baranov, V.; Bohme, D. K. *Tetrahedron* **1996**, *52*, 5191.

(7) (a) Guo, B. C.; Castleman, A. W. *J. Am. Soc. Mass Spectrom.* **1992**, *3*, 464. (b) Guo, B. C.; Castleman, A. W. *J. Am. Chem. Soc.* **1992**, *114*, 6152.

(8) Daly, G. M.; El-Shall, M. S. *J. Phys. Chem.* **1994**, *98*, 696.

(9) Galy, G. M.; Pithawalla, Y. B.; Yu, Z.; El-Shall, M. S. **1995**, *237*, 97.

(10) Forte, L.; Lien, M. H.; Hopkinson, A. C.; Bohme, D. K. *Can. J. Chem.* **1990**, *68*, 1629.

S0002-7863(96)01359-5 CCC: $14.00

ethylene,[11] propylene,[11] *cis*-2-butene,[11] isobutene,[11] and styrene[11] induced by BF_2^+, and with cyanogen induced by Xe^+.[12] There has also been a report of the Fe^+-mediated oligomerization of acetylene.[13] More recently, intracluster ion−molecule reactions have been reported which lead to the cationic polymerization of ethylene,[14] 1,1-difluoroethylene,[14] propene,[14] isoprene,[15] acetylene and propyne,[16] and isobutylene initiated by Al^+ in the presence of $(CH_3)_3CCl$[17] and by Zn^+.[9] Reports of gas-phase addition to multiply-charged cations are less common and less varied, being restricted essentially to the addition, with and without dehydrogenation, of up to three molecules of small hydrocarbons, such as methane, to doubly-charged atomic metal ions such as Ti^{2+}.[18] In our experience, fullerene dications appear to be more highly suited for cation-induced polymerization initiated by multiply-charged cations for several good reasons. In the "ball-and-chain" mechanism (section 1) the C_{60} cage functions as a surface for monomer immobilization and stabilization since it is relatively large and rigid with no internal rotation and widely-spaced vibrational energy levels. Also, Coulombic repulsion acts to promote charge separation and this promotes repeated monomer addition, viz. propagation, at the charge site at the end of the chain. Studies of cation-induced polymerization involving triply-charged cations also have become possible with the discovery of C_{60}. Our recent observation of the multiple addition of acetylene and ethylene to C_{58}^{3+} and C_{60}^{3+} provides the first examples of such polymerization.[6] We are not aware of studies of fullerene−cation induced polymerization in the condensed phase, although persistent singly- and multiply-charged C_{60} cations have now been observed in super acids[19] and there is a rapidly growing literature on neutral polymers incorporating C_{60}.[20]

Here we report our experimental results for the gas-phase chemistry induced by the fullerene cations C_{60}^+, C_{60}^{2+}, and C_{60}^{3+} in allene and propyne. Both of these molecules exhibit an extraordinary capacity for multiple addition to multiply-charged C_{60}, especially allene with C_{60}^{2+} and propyne with C_{60}^{3+}. The kinetics for the multiple addition is carefully monitored and measured and the structures of the adduct ions are deduced using our newly-developed multi-collision CID technique.[21] The rates of addition of allene to $C_{60}(\text{allene})_n^{2+}$ adducts exhibit a remarkable periodicity which is rationalized in terms of an alternating formation of acyclic and cyclic structures involving a greater and lesser degree of charge localization, respectively.

Experimental Section

The rate-coefficient and product-distribution measurements reported here were performed using a Selected-Ion Flow Tube (SIFT) apparatus which has been described previously.[22] All measurements were taken at 294 ± 2 K and at a helium−buffer gas pressure of 0.35 ± 0.01 Torr. Fullerene cations were generated in the ion source by electron impact ionization (∼50 V for $C_{60}^{\bullet+}$, 80 V for C_{60}^{2+}, 105 V for $C_{60}^{\bullet 3+}$) of fullerene vapor. The fullerene sample (∼90% C_{60}, ∼9% C_{70}) was obtained from Termusa Inc. and was introduced into the ion source without further purification. After being selected with a quadrupole mass filter and injected into the flow tube, the C_{60}^{n+} ions were allowed to thermalize by collisions (ca. 4×10^5) with the He buffer gas atoms prior to entering the reaction region. Reactant neutrals were admitted into the flow tube as pure gases. All gases were obtained commercially and were of high purity (generally >99%). The products of reaction were monitored with a second quadrupole mass filter downstream. The data were analyzed in the usual manner.[22] The rate coefficients for primary reactions reported here are estimated to have an uncertainty of ±30%. Higher-order rate coefficients were obtained by fitting the experimental data to the solutions of the system of differential equations for a chain of successive reactions. The accuracy for these fitting procedures depends on several parameters and is reported separately for every calculated high-order rate coefficient.

We have recently modified the operation of our SIFT apparatus for measurements of the collision-induced dissociation (CID) of the sampled ions.[21] In such measurements the downstream nose cone is biased with respect to the flow tube from 0 to −80 V. After traversing the nose-cone orifice, the sampled ions are exposed to a series of electric fields including a front-lens voltage (U_{fl} = 0 to −500 V), a quadrupole field (RF/DC) and an exit-lens voltage (U_{el} = 0 to −500 V). The nose-cone voltages U_{nc}, U_{fl}, and U_{el} are varied using a computer-controlled power supply (Model TD9500, Spectrum Solutions Inc.). U_{nc} is used as a reference voltage while U_{fl} and U_{el} were varied in such a way so as to ensure constant ion-signal ratios I_i/I_Σ, where I_i are the observed ion intensities and I_Σ is the sum of the detected ions. The voltages required to maintain constant ion-signal ratios were determined manually, parametrized, and incorporated into the control program for the power supply. Ion-signal ratios for the ions Ar^+/Fe^+ and $Fe^+/C_{60}^+/(C_{60})Fe^+$ were used for adjustment and calibration in helium buffer/collision gas. These ratios could be kept constant within 1−3% over a range in U_{nc} from 1 to −80 V. This novel SIFT-CID technique has now been applied succesfully in our laboratory to the collisional dissociation of a large variety of ions with a range in bond energies from <20 up to ca. 100 kcal mol^{-1}.[21]

Results and Discussion

Table 1 provides a summary of the measured rate coefficients and product distributions for the primary reactions of $C_{60}^{\bullet+}$, C_{60}^{2+}, and C_{60}^{3+} with allene and propyne. Those for the higher-order reactions are included in the following text.

I. Reactions with Allene. The singly-charged cation $C_{60}^{\bullet+}$ was found to be unreactive toward allene, $k_1 \leq 1 \times 10^{-14}$ cm^3 $molecule^{-1}$ s^{-1}:

$$C_{60}^{\bullet+} + \text{allene} \rightarrow \text{no reaction} \qquad (3)$$

Electron transfer is endothermic for reaction 3 since the ionization energy of C_{60}, $IE(C_{60}) = 7.64 \pm 0.02$ eV,[23] is smaller than the ionization energy of allene, $IE(\text{allene}) = 9.69 \pm 0.01$ eV.[24] Also, nucleophilic addition of the allene to $C_{60}^{\bullet+}$ is not expected due to the low strength of this cation as a Lewis acid. We have found previously that $C_{60}^{\bullet+}$ is generally quite unre-

(11) (a) Forte, L.; Lien, M. H.; Hopkinson, A. C.; Bohme, D. K. *Makromol. Chem., Rapid Commun.* **1987**, *8*, 87. (b) Forte, L.; Lien, M. H.; Hopkinson, A. C.; Bohme, D. K. *Can. J. Chem.* **1989**, *67*, 1576.

(12) Raksit, A. B.; Bohme, D. K. *Can. J. Chem.* **1984**, *62*, 2123.

(13) Schröder, D.; Detlev, S.; Hrusak, J.; Bohme, D. K.; Schwarz, H. *Int. J. Mass Spectrom. Ion Processess* **1991**, *110*, 145.

(14) Coolbaugh, M. T.; Waidynanathan, G.; Peifer, W. R.; Garvey, J. F. *J. Phys. Chem.* **1991**, *95*, 8337.

(15) El-Shall, M. S.; Marks, C. *J. Phys. Chem.* **1991**, *95*, 4932.

(16) Coolbaugh, M. T.; Whithney, S. G.; Vaidyanathan, G.; Garvey, J. F. *J. Phys. Chem.* **1992**, *96*, 9139.

(17) Daly, G. M.; El-Shall, M. S. *J. Phys. Chem.* **1995**, *99*, 5283.

(18) Roth, L. M.; Freiser, B. S. *Mass Spectrom. Rev.* **1991**, *10*, 303.

(19) (a) Kukolich, S. G.; Huffman, D. R *Chem. Phys. Lett.* **1991**, *182*, 263. (b) Thomann, H.; Bernardo, M.; Miller, G. P. *J. Am. Chem. Soc.* **1992**, *114*, 6593. (c) Miller, G. P.; Hsu, C. S.; Thomann, H.; Chiang, L. Y.; Bernardo, M. *Mater. Res. Soc. Symp. Proc.* **1992**, *247*, 293.

(20) See, for example: (a) Loy, D. A.; Assink, R. A. *J. Am. Chem. Soc.* **1992**, *114*, 3977. (b) Geckeler, K. E.; Hirsch, A. *J. Am. Chem. Soc.* **1993**, *115*, 3850. (c) Rao, A. M.; Zhou, P.; Wang, Kai-An; Hager, G. T.; Holden, J. M.; Wang, Y.; Lee, W.-T.; Bi, Xiang-Xin; Eklund, P. C.; Cornett, D. S.; Duncan, M. A.; Amster, I. J. *Science* **1993**, *259*, 955. (d) Tanaka, K.; Matsuura, Y.; Oshima; Yamabe, T. *Chem. Phys. Lett.* **1995**, *237*, 127. (e) Dal, L.; Mao, A. W. H.; Griesser, H. J.; Spurling, T. H.; White, J. W. *J. Phys. Chem.* **1995**, *99*, 17302.

(21) Baranov, V.; Bohme, D. K. *Int. J. Mass Spectrom. Ion Processes* **1996**, *154*, 71.

(22) (a) Mackay, G. I.; Vlachos, G. D.; Bohme, D. K.; Schiff, H. I. *Int. J. Mass Spectrom. Ion Phys.* **1980**, *36*, 259. (b) Raksit, A. B.; Bohme, D. K. *Int. J. Mass Spectrom. Ion Processes* **1983**, *55*, 69.

(23) Lichtenberg, D. L.; Rempe, M. E.; Gogosha, S. B. *Chem. Phys. Lett.* **1992**, *198*, 454.

(24) Lias, S. G.; Bartmess, J. E.; Liebman, J. F.; Holmes, J. L.; Levin, R. D.; Mallard, W. G. *J. Phys. Chem. Res. Data* **1988**, *17*, 1.

Table 1. Measured Rate Coefficients for Reactions of C_{60}^{x+} (x = 1, 2, and 3) with Allene and Propyne in the Gas Phase at 294 ± 3 K and at a Helium Buffer Gas Pressure of 0.35 ± 0.01 Torr

ion	k_{obs}[a]	k_{cap}[b]
	Reactions with Allene	
C_{60}^{+}	$<10^{-14}$	9.3×10^{-8}
C_{60}^{2+}	3.1×10^{-11}	1.9×10^{-9}
$C_{60}(C_3H_4)_n^{2+}$		
$n = 1$	$1.8 \pm 0.4 \times 10^{-12}$	1.9×10^{-9}
$n = 2$	$2.5 \pm 1.5 \times 10^{-11}$	1.9×10^{-9}
$n = 3$	$<4 \times 10^{-12}$	1.8×10^{-9}
C_{60}^{3+} (CT 100%)	4.0×10^{-9}	2.8×10^{-9}
	Reactions with Propyne	
C_{60}^{+}	$<10^{-14}$	1.2×10^{-9}
C_{60}^{2+}	1.6×10^{-10}	2.3×10^{-9}
$C_{60}(C_3H_4)_n^{2+}$		
$n = 1$	$2.9 \pm 0.5 \times 10^{-11}$	2.3×10^{-9}
$n = 2$	$4.0 \pm 1.1 \times 10^{-12}$	2.3×10^{-9}
$n = 3$	$<5.0 \times 10^{-13}$	2.3×10^{-9}
C_{60}^{3+} (CT 25%)	1.8×10^{-9}	3.5×10^{-9}
$C_{60}(C_3H_4)_n^{3+}$		
$n = 1$	$1.5 \pm 0.5 \times 10^{-9}$	3.5×10^{-9}
$n = 2$	$1.3 \pm 0.4 \times 10^{-9}$	3.5×10^{-9}
$n = 3$	$2.0 \pm 1.0 \times 10^{-9}$	3.5×10^{-9}

[a] Measured effective bimolecular reaction-rate coefficient in units of cm^3 $molecule^{-1}$ s^{-1}. The absolute error may be as high as ±30% for the primary reactions. The standard error introduced by the fitting procedure is indicated for the higher-order reactions. [b] The collision rate coefficient was calculated according to the ADO theory (ref 36).

active and only barely adds to strong Lewis bases such as ammonia and aliphatic amines in the gas phase.[25]

Experimental results for the reaction of C_{60}^{2+} with allene are shown in Figure 1. Association was the only product channel observed as is indicated in reaction 4. The effective bimolecular

$$C_{60}^{2+} + \text{allene} \rightarrow C_{60}(C_3H_4)^{2+} \quad (4)$$

rate coefficient for this reaction was measured to be 3.1×10^{-11} cm^3 $molecule^{-1}$ s^{-1} . Electron transfer was observed not to compete with the association reaction even though it is exothermic. The ionization energy of $C_{60}^{\bullet+}$, IE($C_{60}^{\bullet+}$), is 11.36 ± 0.05 eV[26,27] and the exothermicity of electron transfer is only 1.7 eV, which is just below the threshold associated with an energy barrier of 1.8 ± 0.16 eV[27,28] which arises from Coulombic repulsion between the singly-charged product ions of the electron-transfer reaction.

Figure 1 shows that $C_{60}(C_3H_4)^{2+}$ continues to react with allene in the flow tube and sequentially forms the adducts $C_{60}(C_3H_4)_n^{2+}$ according to reaction 5 where n was detected in the range from

$$C_{60}(C_3H_4)_n^{2+} + \text{allene} \rightarrow C_{60}(C_3H_4)_{n+1}^{2+} \quad (5)$$

1 up to 15. A most remarkable feature of this sequential addition is the periodicity in the reactivity of the adduct ions: the reactivities of the odd-numbered adduct ions are systematically lower than the reactivities of the succeeding even-numbered adduct ions, by a factor of about 10 judging from the relative magnitudes of the odd- and even-numbered adduct ions. This multi-addition of allene to C_{60}^{2+} most likely proceeds by termolecular association under our operating conditions with

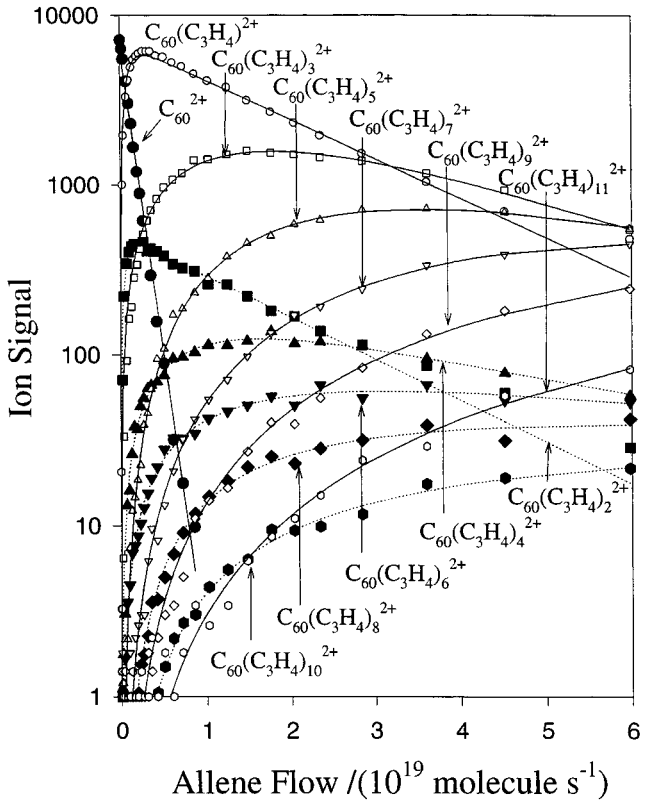

Figure 1. Experimental data for the reaction of C_{60}^{2+} with allene. Only adducts are shown. The odd adducts are presented by open symbols and solid lines, the even adducts by closed symbols and dotted lines. The measurements were performed at 294 ± 3 K and at a helium buffer-gas pressure of 0.35 ± 0.01 Torr. The lines for the first, second, and third adducts represent a fit of the experimental data with the solution of the system of differential equations appropriate for the observed sequential reactions. Rate coefficients derived from this fit are given in Table 1. All other lines were drawn for clarity.

He atoms acting as the stabilizing third body, but we cannot rule out radiative association as a significant contribution to the mechansim of addition,[29] particularly for the larger adduct ions. We did not investigate the pressure dependence of reaction 5.

Our observations at higher flows of allene, shown in Figure 2, indicate that two bimolecular reactions compete with, and therefore act to terminate, the sequential association of allene. Reaction 6 sets in at $n = 1$ for which it is only a minor channel,

$$C_{60}(C_3H_4)_n^{2+} + \text{allene} \rightarrow C_{60}(C_3H_4)_{n-1}H^{+} + C_6H_7^{+} \quad (6)$$

<10%. Both $C_{60}H^{+}$ and $C_6H_7^{+}$ were observed as product ions for $n = 1$. Also, we have found that the rise in the $C_9H_{12}^{+}$ signal ($m/z = 120$) coincides with the fall in the $C_{60}(C_3H_4)_4^{2+}$ signal (see Figure 2) and corresponds to the onset at $n = 3$ of the bimolecular reaction 7. We note that the resolution of our

$$C_{60}(C_3H_4)_n^{2+} + \text{allene} \rightarrow C_{60}(C_3H_4)_{n-2}^{+} + C_9H_{12}^{+} \quad (7)$$

analyzing mass spectrometer and the low signal intensity did not allow us to distinguish between the $C_{60}(C_3H_4)_{n-1}H^{+}$ and $C_{60}(C_3H_4)_{n-2}^{+}$ signals produced by reaction 6 for $n > 1$ and by reaction 7, respectively, but that the concomitant formation of $C_6H_7^{+}$ and $C_9H_{12}^{+}$ could easily be characterized.

(25) Javahery, G.; Petrie, S.; Wincel, H.; Bohme, D. K. *J. Am. Chem. Soc.* **1993**, *115*, 5716.
(26) Steger, H.; de Vries J.; Kamke, B.; Kamke, W.; Drewello T. *Chem. Phys. Lett.* **1992**, *194*, 452.
(27) Bohme, D. K. *Int. Rev. Phys. Chem.* **1994**, *13*, 163.
(28) Petrie, S.; Javahery, G.; Wang, J.; Bohme, D. K. *J. Phys. Chem.* **1992**, *96*, 6121.
(29) (a) Herbst, E.; Dunbar, R. C. *Mon. Not. R. Astron. Soc.* **1991**, *253*, 341. (b) Dunbar, R. C. *Mass Spectrom. Rev.* **1992**, *11*, 309−339.

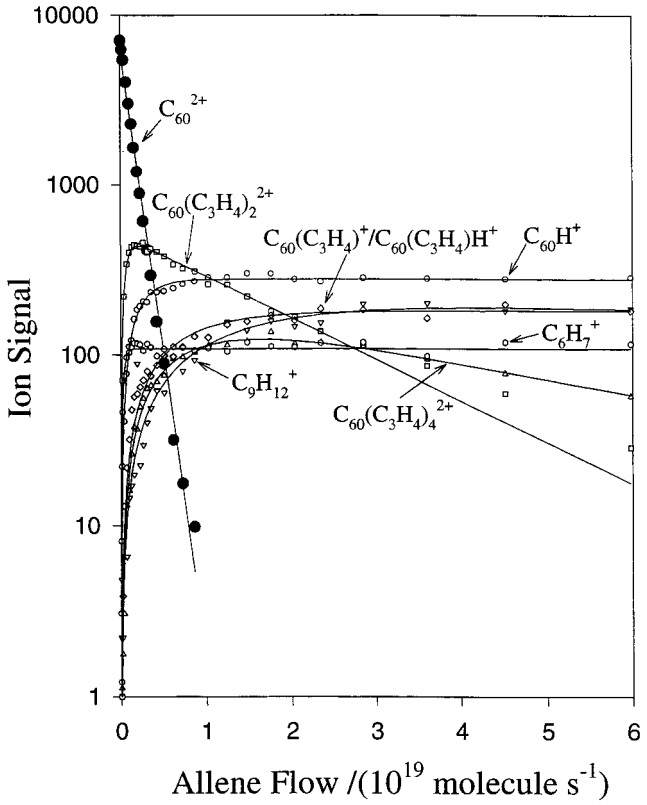

Figure 2. The primary ion decay and profiles for other selected product ions observed along with the experimental results shown in Figure 1. The reaction profiles for C_{60}^{2+} and $C_{60}(C_3H_4)_2^{2+}$ represent a fit to the experimental data. All other lines are drawn for clarity.

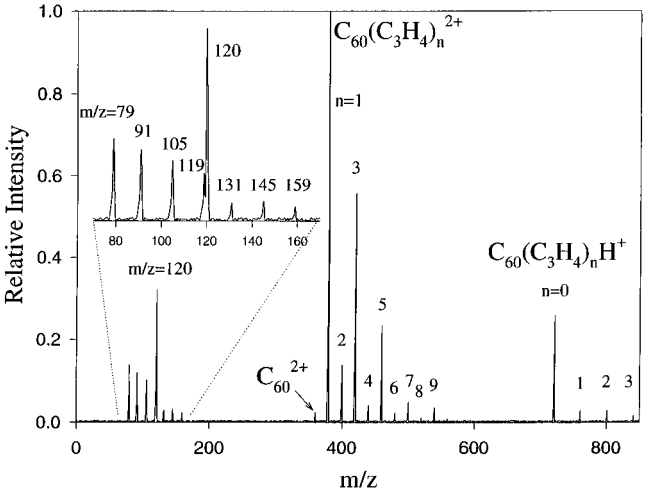

Figure 3. A typical mass spectrum recorded for the addition of allene to C_{60}^{2+}. The allene flow is 2.3×10^{19} molecule s^{-1}, T = 294 ± 3 K, the helium buffer-gas pressure is 0.35 ± 0.01 Torr, and the mean bulk gas velocity is 4.7×10^3 cm s^{-1}.

Figure 3 gives an impression of the extensive allene-ion chemistry initiated by the $C_6H_7^+$ generated in reaction 6. Allene-ion chemistry has been explored extensively in the past using high-pressure ion-source mass spectrometry,[30] ICR,[31−33] and photoionization mass spectrometry,[32] but apparently never under SIFT conditions. These earlier studies have established that $C_6H_7^+$ can be formed by reaction 8 and that this ion reacts further with allene to generate $C_7H_7^+$ (m/z = 91) and $C_9H_{11}^+$

$$C_3H_4^+ + \text{allene} \rightarrow C_6H_7^+ + H \qquad (8)$$

(m/z = 119), but did not provide information on higher-order allene-ion chemistry. We briefly investigated the higher-order allene-ion chemistry in separate SIFT experiments which showed that the allene-ion chemistry initiated by $C_6H_7^+$ produced in reaction 6 matches that of $C_6H_7^+$ produced by reaction 8. The production of the ions in Figure 3 with m/z = 91, 105, 119, 131, 145, and 159 is consistent with the following reaction scheme:

$$C_6H_7^+ + \text{allene} \rightarrow C_7H_7^+ + C_2H_4 \qquad (9)$$

$$C_7H_7^+ + \text{allene} \rightarrow C_{10}H_{11}^+ (m/z = 131) \qquad (10a)$$

$$\rightarrow C_8H_9^+ (m/z = 105) + C_2H_2 \qquad (10b)$$

$$C_8H_9^+ + \text{allene} \rightarrow C_{11}H_{13}^+ (m/z = 145) \qquad (11a)$$

$$\rightarrow C_9H_{11}^+ (m/z = 119) + C_2H_2 \qquad (11b)$$

$$C_9H_{11}^+ + \text{allene} \rightarrow C_{12}H_{15}^+ (m/z = 159) \qquad (12)$$

The overall chemistry initiated by C_{60}^{2+} in allene under our SIFT conditions is summarized in Scheme 1.

Allene was observed to react rapidly with C_{60}^{3+} solely by electron transfer according to reaction 13. This result is not

$$C_{60}^{3+} + \text{allene} \rightarrow C_{60}^{2+} + C_3H_4^+ \qquad (13)$$

surprising since electron-transfer bracketing measurements have established an ionization energy threshold for electron transfer to C_{60}^{3+} of 11.09 ± 0.09 eV which exceeds IE(allene) by 1.4 eV.[34] The secondary chemistry of C_{60}^{2+} and $C_3H_4^+$ was observed to be identical to that discussed in the previous section.

II. Reactions with Propyne. As was the case with allene, propyne also does not react with the singly-charged cation C_{60}^+.

Scheme 1

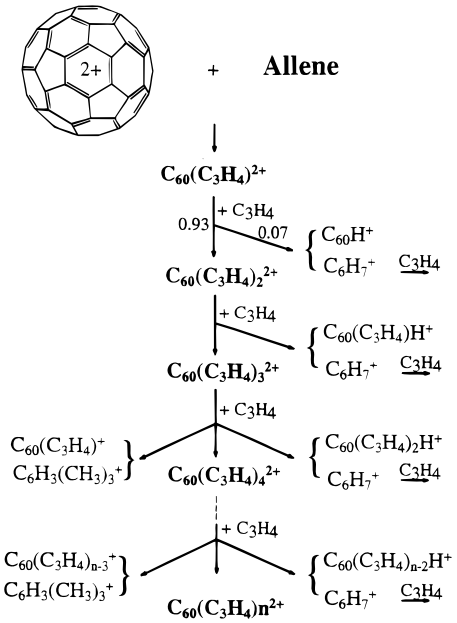

(30) Myher, J. J.; Harrison, A. G. *J. Phys. Chem.* **1968**, *72*, 1905.
(31) Anicich, V. G.; Geoffrey, A. B.; Kim, J. K.; McEwan, M. J.; Huntress, W. T. *J. Phys. Chem.* **1984**, *88*, 4608.
(32) Lifshitz, C.; Gleitman, Y.; Gefen, S.; Shainok, U. *Int. J. Mass Spectom. Ion Phys.* **1981**, *40*, 1.
(33) Lias, S. G.; Ausloos, P. J. *Chem. Phys.* **1985**, *82*, 3612.
(34) Javahery, G.; Wincel, H.; Petrie, S.; Bohme, D. K. *Chem. Phys. Lett.* **1993**, *204*, 467.

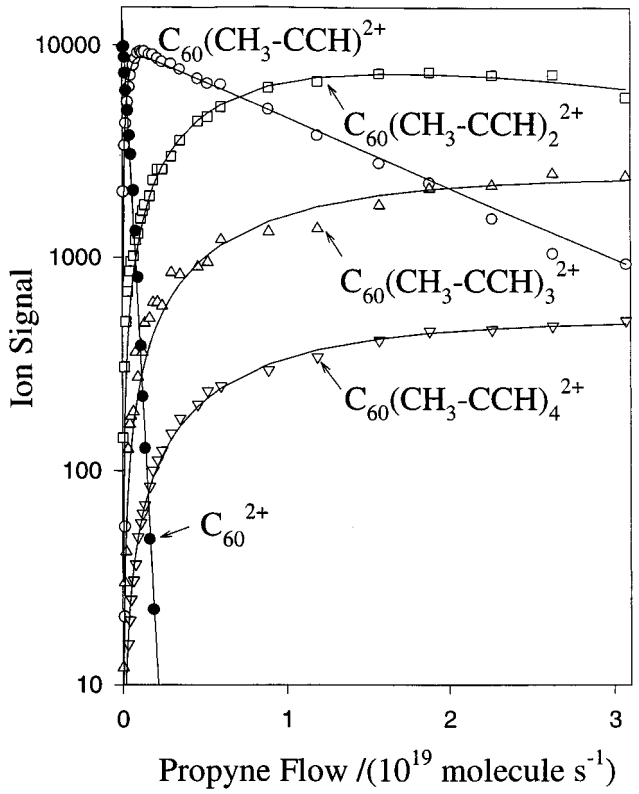

Figure 4. Experimental data for the reaction of C_{60}^{2+} with propyne. The measurements were performed at 294 ± 3 K and at a helium buffer-gas pressure of 0.35 ± 0.01 Torr. The lines for the adducts represent a fit of the experimental data with the solution of the system of differential equations appropriate for the observed sequential reactions. Rate coefficients derived from this fit are given in Table 1.

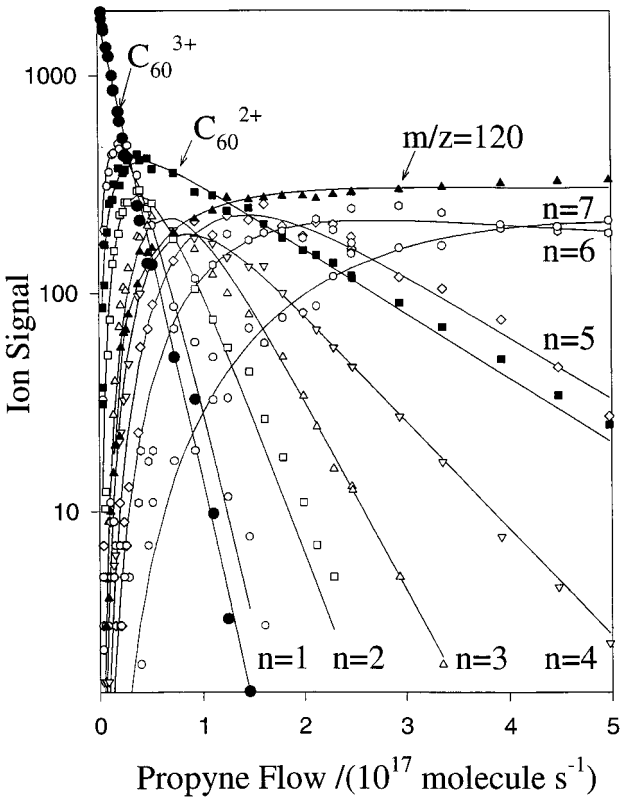

Figure 5. Experimental data for the reaction of C_{60}^{3+} with propyne. The measurements were performed at 294 ± 3 K and at a helium buffer-gas pressure of 0.35 ± 0.01 Torr. The dotted lines for the first, second, and third adducts represent a fit of the experimental data with the solution of the system of differential equations appropriate for the observed sequential reactions. Rate coefficients derived from this fit are given in Table 1. All other dotted lines were drawn for clarity. Here *n* indicates the number of propyne adduct molecules in $C_{60}(C_3H_4)_n^{3+}$.

The rate coefficient for reaction 14 was determined to be ≤1

$$C_{60}^{+} + \text{propyne} \rightarrow \text{no reaction} \qquad (14)$$

× 10^{-14} cm^3 $molecule^{-1}$ s^{-1}. Electron transfer again is endothermic, given the relatively high ionization energy of propyne, IE(propyne) = 10.36 ± 0.01 eV.[24]

Figure 4 shows that the addition reaction 15

$$C_{60}^{2+} + \text{propyne} \rightarrow C_{60}(C_3H_4)^{2+} \qquad (15)$$

was the only reaction observed between propyne and C_{60}^{2+} and it was found to occur quite rapidly under our experimental operating conditions, $k_{15} = 1.6 \times 10^{-10}$ cm^3 $molecule^{-1}$ s^{-1}. Electron transfer was not detected as a competing reaction. Although the ionization energy of C_{60}^{+} is higher than that for propyne, the exothermicity for electron transfer is only 1.0 eV, which is significantly lower than the threshold associated with an energy barrier of 1.8 ± 0.16 eV,[27,28] which arises from Coulombic repulsion between the singly-charged product ions of the electron-transfer reaction.

Our experimental observations of the higher-order chemistry initiated by C_{60}^{2+} in propyne shown, in part, in Figure 4 indicate the occurrence of the sequence of addition reactions described by reaction 16 for *n* up to 5. Competing channels

$$C_{60}(C_3H_4)_n^{2+} + \text{propyne} \rightarrow C_{60}(C_3H_4)_{n+1}^{2+} \qquad (16)$$

analogous to reactions 6 and 7, which produced $C_6H_7^{+}$ and $C_9H_{12}^{+}$ in allene, were not observed with propyne. A computer fit to the experimental data for *n* up to 3 indicated a steady decrease in the magnitude of k_{16} by a factor of at least 7 for *n* ≥ 1 (see Table 1). Also, it should be noted that, in contrast to the observations with isomeric allene, there is no obvious periodicity in the higher-order sequential addition of propyne.

Chemistry initiated by C_{60}^{3+} with propyne is shown in Figure 5. The first step in this chemistry is 11 times faster than that observed with C_{60}^{2+}, $k_{17} = 1.8 \times 10^{-9}$ cm^3 $molecule^{-1}$ s^{-1}, and involves both association, channel 17a, and electron transfer, channel 17b. The branching ratio was determined to be 0.75/0.25 in favor of association. The electron transfer channel is sufficiently exothermic to overcome the energy barrier arising from Coulombic repulsion between the singly-charged product ions. IE(propyne) lies 0.7 eV below the ionization energy threshold previously determined for electron-transfer reactions with C_{60}^{3+}.[34]

$$C_{60}^{3+} + \text{propyne} \rightarrow C_{60}(C_3H_4)^{3+} \qquad (17a)$$

$$\rightarrow C_{60}^{2+} + C_3H_4^{+} \qquad (17b)$$

As shown in Figure 5, the formation of the adduct ion $C_{60}(C_3H_4)^{3+}$ in reaction 15a is the first step in a sequence of rapid addition reactions given by reaction 18 which we have observed

$$C_{60}(C_3H_4)_n^{3+} + \text{propyne} \rightarrow C_{60}(C_3H_4)_{n+1}^{3+} \qquad (18)$$

for *n* up to 6. The data indicate that the rate of this reaction decreases with increasing *n* by less than a factor of 2 for each

step and there is no significant discontinuity after the addition of the first propyne molecule. Computer fits have provided the rate coefficients for the first few steps which are listed in Table 1. Figure 5 shows clearly the onset of a product ion with $m/z = 120$ signal after the addition of three propyne molecules and this signal continues to grow with the number of propyne molecules added to C_{60}^{3+}. We attribute the formation of the $m/z = 120$ ion to the occurrence of the bimolecular reaction 19

$$C_{60}(C_3H_4)_n^{3+} + \text{propyne} \rightarrow C_{60}(C_3H_4)_{n-2}^{2+} + C_9H_{12}^{+} \quad (19)$$

which is the analogue of reaction 7 observed between C_{60}^{2+} and allene. The analogue of reaction 6 observed between C_{60}^{2+} and allene which leads to $C_6H_7^+$ was not observed to compete with reaction 18.

The propyne reactions of the C_{60}^{2+} cation produced in the electron-transfer reaction 17b were observed to be similar to those described above for C_{60}^{2+} produced from C_{60} by electron impact in the ion source. The $C_3H_4^+$ ion produced in reaction 17b also reacted further with propyne, initially to form $C_6H_7^+$ in the well-known reaction 20.[30−33] The $C_6H_7^+$ then reacted

$$C_3H_4^{+} + \text{propyne} \rightarrow C_6H_7^{+} + H \quad (20)$$

further by sequentially adding at least two propyne molecules according to reaction 21. It is interesting to note the absence

$$C_6H_7^{+}\cdot(\text{propyne})_n + \text{propyne} \rightarrow C_6H_7^{+}\cdot(\text{propyne})_{n+1} \quad (21)$$

of the analogues of the C_2H_2-elimination channels 10b and 11b leading to the formation of ions with $m/z = 105$ and 119 observed in the allene chemistry.

III. Structures of Adduct Ions. There are a number of possible structures for the allene and propyne adduct ions which were observed with C_{60}^{2+} and C_{60}^{3+}. These include the "fuzzy ball", "spindle", and "ball-and-chain" structures depicted below as structures **I**, **II**, and **III**, respectively. These structures may arise from sequential addition on the surface of C_{60}, sequential addition at the sites of charge (two in the case of C_{60}^{2+}), and sequential addition at one charge site, respectively. Insight into the actual structures of the adduct ions observed in our experiments was obtained with our newly-developed CID technique,[21] which we have recently applied to the exploration of the structures of multiple adducts of 1-butene with C_{60}^{2+}.[5]

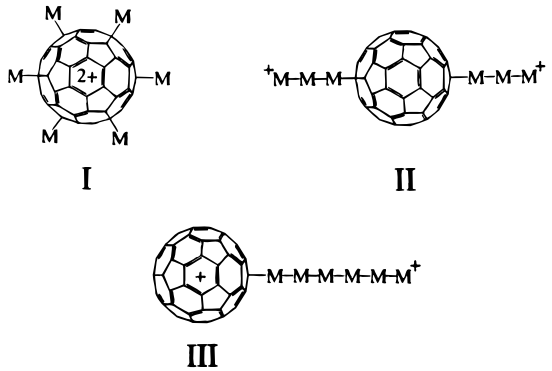

A multiple-collision CID spectrum for the single and multiple adducts of allene is shown in Figure 6. Dissociation was observed for all adduct ions. Only $C_{60}^{\bullet+}$ and C_{60}^{2+} were observed as C_{60}-containing product ions. The production of C_{60}^{2+} is due solely to the dissociation of the first adduct. This was confirmed in separate experiments in which $C_{60}(CH_2{=}C{=}CH_2)^{2+}$ was established as the dominant ion in the CID region. The production of $C_{60}^{\bullet+}$ is due solely to the

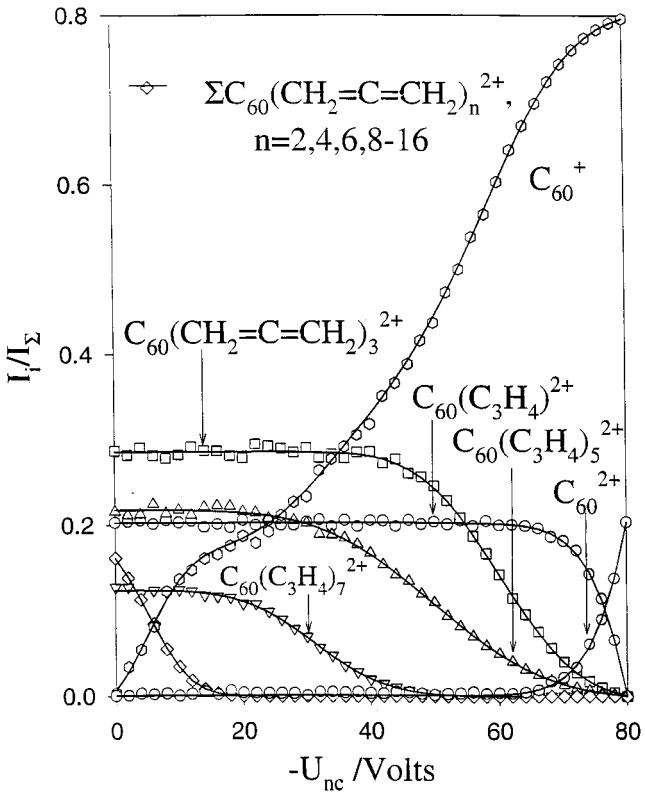

Figure 6. Measured profiles for the multi-collision-induced dissociation of $C_{60}(\text{allene})_n^{2+}$ with $n = 2$, 4, 6, and 8−16. The allene flow, 4.5×10^{19} molecules s^{-1}, was chosen to maximize the extent of addition in 10% argon/helium buffer/collision gas at a total pressure of 0.30 ± 0.01 Torr and a temperature of 294 ± 3 K. The C_{60}^{2+} was generated in a low-pressure ion source by electron impact ionization at 80 eV of C_{60} vapor derived from heated fullerene powder.

dissociation of all the higher adduct ions. The concomitant production of $(C_3H_4)_n^+$ ions was also observed, but only for $n \leq 5$, since they themselves undergo further collisional dissociation.[5] We have interpreted these results to indicate two types of dissociative behavior. The monoadduct dissociates at the fullerene surface according to eq 22 to produce C_{60}^{2+} by

$$C_{60}(CH_2{=}C{=}CH_2)^{2+} + Ar \rightarrow C_{60}^{2+} + C_3H_4 + Ar \quad (22)$$

eliminating a neutral molecule, while the multiple adducts ($n = 2$ to 16) dissociate at the fullerene surface into two singly-charged cations according to eq 23.

$$C_{60}(CH_2{=}C{=}CH_2)_n^{2+} + Ar \rightarrow C_{60}^{+} + (C_3H_4)_n^{+} + Ar \quad (23)$$

A multiple-collision CID spectrum for the single and multiple adducts of propyne to C_{60}^{2+} is shown in Figure 7. In this case, only dissociation to produce C_{60}^{2+} according to reaction 24 was

$$C_{60}(CH_3C{\equiv}CH)_n^{2+} + Ar \rightarrow C_{60}^{2+} + (C_3H_4)_n + Ar \quad (24)$$

observed for $n = 1$ to 4. Since the neutral products could not be detected, it was not possible to establish unequivocally whether the neutral fragments as monomers or oligomers.

A multiple-collision CID spectrum for the single and multiple adducts of propyne to C_{60}^{3+} is shown in Figure 8. Only dissociation to produce C_{60}^{3+} according to reaction 25 was observed for $n = 1$ to 3. Again, it was not possible to establish

$$C_{60}(CH_3C{\equiv}CH)_n^{3+} + Ar \rightarrow C_{60}^{3+} + (C_3H_4)_n + Ar \quad (25)$$

the state of aggregation of the neutral products.

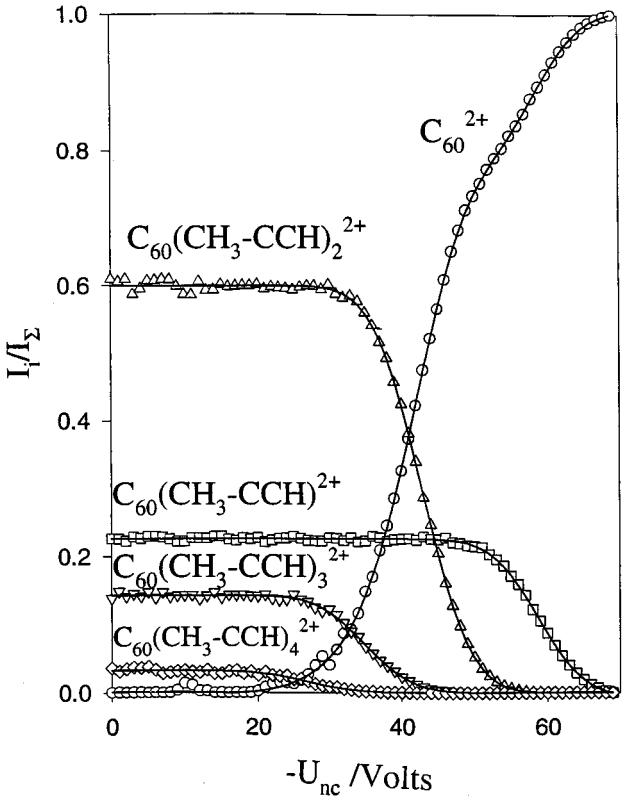

Figure 7. Measured profiles for the multi-collision-induced dissociation of $C_{60}(propyne)_n^{2+}$ with $n = 1$, 2, 3, and 4. The propyne flow, 1.5×10^{19} molecules s^{-1}, was chosen to maximize the extent of addition in 10% argon/helium buffer/collision gas at a total pressure of 0.30 ± 0.01 Torr and a temperature of 294 ± 3 K. The C_{60}^{2+} was generated in a low-pressure ion source by electron impact ionization at 80 eV of C_{60} vapor derived from heated fullerene powder.

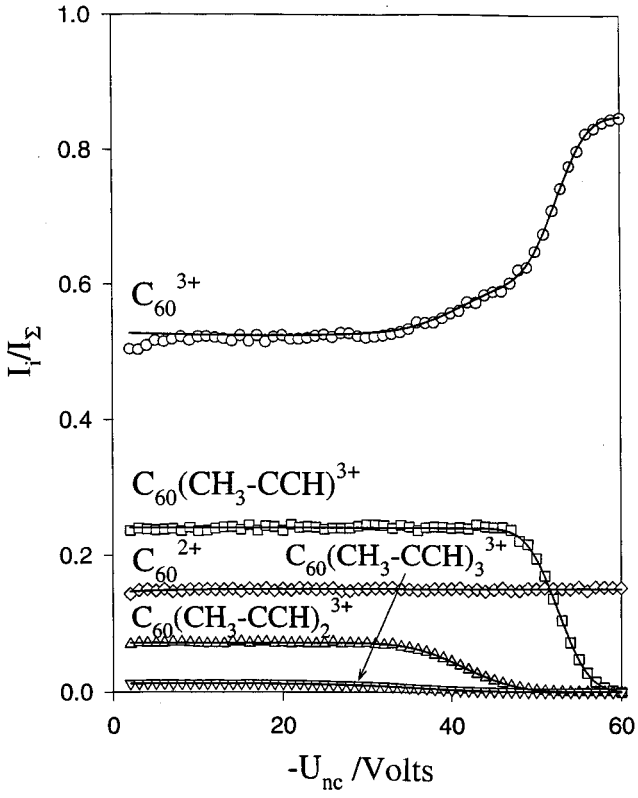

Figure 8. Measured profiles for the multi-collision-induced dissociation of $C_{60}(propyne)_n^{3+}$ with $n = 1$, 2, and 3. The propyne flow was 2×10^{16} molecules s^{-1}. Reaction and dissociation occurred in 10% argon/helium buffer/collision gas at a total pressure of 0.30 ± 0.01 Torr and a temperature of 294 ± 3 K. The C_{60}^{2+} was generated in a low-pressure ion source by electron impact ionization at 80 eV of C_{60} vapor derived from heated fullerene powder.

The observation of the total removal of the adduct molecules either as neutrals or ions and the failure to observe removal of single molecules in the dissociation of the multiple-adduct ions favor a "ball-and-chain" structure over a "spindle" or "fuzzy-ball" structure for the $C_{60}M_n^{x+}$ ($x = 2$, 3) adduct ions observed. We view the two types of dissociation which were observed as heterolytic dissociation, channel 26a, and homolytic dissociation, channel 26b. Given the relative magnitudes of $IE(C_{60}^{(x-1)+})$

$$C_{60}(M_n)^{x+} + Ar \rightarrow C_{60}^{x+} + (M_n) + Ar \quad (26a)$$

$$\rightarrow C_{60}^{(x-1)+} + (M_n)^+ + Ar \quad (26b)$$

and $IE(M_n)$, we expect the latter channel to be less endothermic for $x = 2$ or 3 and M = allene or propyne. The charge-separation channel 26b involves a transition between a bound state and a Coulombic repulsive potential-energy curve. Such a transition has been modeled for $n = 1$ by Petrie et al.[28] in terms of an effective energy barrier for the formation of the two product cations. If the barrier for homolytic cleavage for $n = 1$ lies above the dissociation limit for heterolytic cleavage, it could drop below the dissociation limit for heterolytic cleavage as n increases. This is possible since the *difference* in the endothermicities of (26a) and (26b) should increase with n because M_n^+ is stabilized more by the addition of an M molecule than is M_n (although the increments should decrease in magnitude as n increases). Such a trend would account for the change from heterolytic to homolytic dissociation observed with the allene adducts $C_{60}(allene)_n^{\bullet+}$ beyond $n = 1$ if the additon of one molecule of allene were enough to reduce the barrier for homolytic dissociation below the energy of the heterolytic dissociation. For the propyne adducts, $C_{60}(propyne)_n^{2+}$ and $C_{60}(propyne)_n^{\bullet 3+}$, heterogeneous dissociation is always observed to be the preferred path of dissociation. Presumably, in the case of the dissociation of $C_{60}(propyne)_n^{2+}$, this is because the barrier for homolytic dissociation never falls below the energy of the heterolytic dissociation limit. Indeed, the difference in endothermicity of channels 26a and 26b is smaller for $n = 1$ in the case of the dissociation of $C_{60}(propyne)_n^{2+}$ because of the higher ionization energy of propyne. In the case of the homolytic dissociation of $C_{60}(propyne)_n^{\bullet 3+}$ the difference in endothermicity of channels 26a and 26b is again larger for $n = 1$ because of the higher ionization energy of C_{60}^{2+}, but the Coulombic barrier is also larger.

We also note a dependence of the onset for dissociation on the number of molecules added to the $C_{60}M_n^{2+}$ cation, namely that the onset moves to lower voltages with an increase in the number of molecules added. Furthermore, the adduct ions with an even number of attached allene molecules uniformly have a lower onset for dissociation than those with an odd number of attached allene molecules, even though the same bond, viz. the bond at the C_{60} surface, appears to be broken. This latter behavior implies a lower stability for $C_{60}M_n^{2+}$ against dissociation into C_{60}^+ and M_n^+ with even n. Several factors can contribute to the general trend of decreasing onset voltage for the dissociation of $C_{60}M_n^{2+}$ with increasing n including differences in stability and differences in energy transfer arising from differences in mass, size, and number of degrees of freedom of the $C_{60}M_n^{2+}$ cation. With regard to the former, we can expect the $^+C_{60}-M_n^+$ bond to be more easily broken for larger n since the reduction in Coulombic repulsion between the products results in a lower effective barrier to dissociation for larger n;

Scheme 2

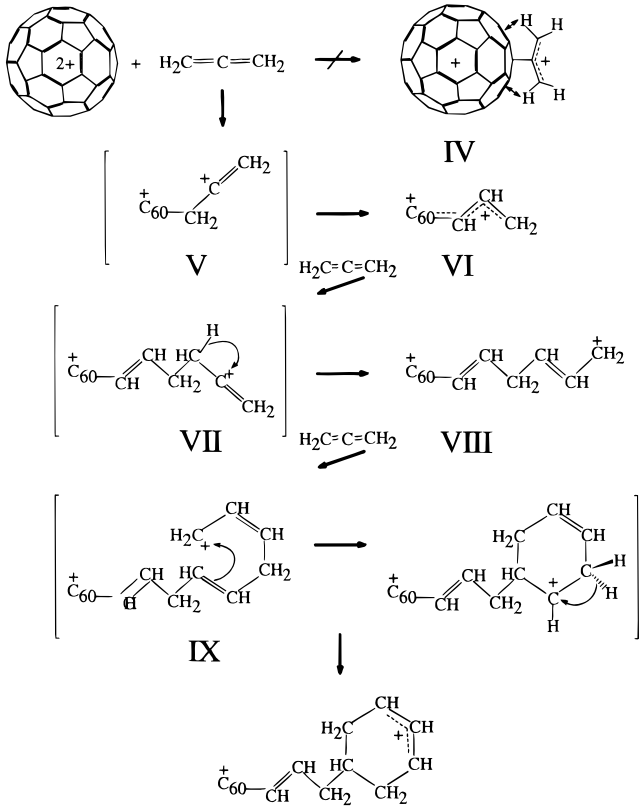

M_n^+ itself is also a more stable product for larger *n*. With regard to the latter, we can expect the probability for bond dissociation *under multiple-collision conditions* to increase with the number of degrees of freedom because of the increase in total internal energy accompanying the increase in the number of degrees of freedom of $C_{60}M_n^{2+}$. A higher probability of dissociation will translate into a lower measured onset for dissociation. Also, the concomitant increase in size should lead to an increase in the cross section for energy transfer.

IV. Mechanisms for C_{60} Cation-Induced Polymerization. The remarkable periodicity observed for the sequential addition of allene to C_{60}^{2+} may be explained in terms of the mechanism proposed in Scheme 2. Initial electrophilic addition to C_{60}^{2+} at either the electron-rich central carbon atom or the terminal carbon atom in allene would form either the allyl cation **IV** or the vinyl cation **V**, respectively. In both cases, C−C covalent bond formation would be accompanied by a change in the hybridization of the bonding C atom on the C_{60} cage and the bonding C atom in allene. We suggest that terminal-carbon addition to form the vinyl cation is preferred over central-carbon addition for several reasons. Ion-induced dipole interaction during the collision is expected to lead preferentially to an "end-on" attack since the dipole will be induced along the C−C−C axis of allene. Furthermore, end-on bonding allows the occurrence of a 1,2-hydride shift to form the 1-allyl-substituted structure **VI** in which the charge may be delocalized into the C_{60} cage. Also, the spacial interaction of the terminal hydrogen atoms of allene with the "almost flat" C_{60} surface in a "side-on" collision (see structure **IV**) makes bonding with the central carbon atom of allene sterically unfavorable.

The end-on addition of a second molecule of allene to structure **VI** will lead to structure **VII** in which the charge can again be propagated to the terminal carbon atom through hydride transfer to give the acyclic allyl cation **VIII**. The next addition of allene accompanied by a hydride shift should lead to structure **IX**, which may ring-close to the cyclic allyl structure since the second double bond is susceptible to intramolecular electrophilic attack. (The cyclization of the second adduct **VII** should be less favorable because of the shorter distance between the two separated positive charges.) The subsequent addition of another allene molecule produces an acyclic fourth adduct which forms a cyclic fifth adduct, and so on as shown in Scheme 3. This is consistent with the observed periodicity in the addition kinetics since the cyclic (odd-numbered, $n > 1$) allene adducts are expected to be less reactive than the acyclic (even-numbered) allene adducts because of their greater degree of charge delocalization. Also, a higher stability for the cyclic adducts will enhance their rate of formation.

A possible mechanism for the sequential addition of propyne to C_{60}^{3+} is given in Scheme 4, and this should also be representative of the mechanism for sequential addition to C_{60}^{2+}. We propose that the electrophilic attack of propyne by $C_{60}(\text{propyne})_n^{n+}$ proceeds by bonding with the more negative CH end of this polar molecule as a consequence of dipole alignment, forming a vinyl cation in which the positive charge is partially delocalized by hyperconjugation onto the methyl group attached to the α-carbon. In this mechanism intramolecular cyclization, possibly leading to a periodic depression of the reaction rate, is much less favorable because of charge delocalization along the conjugated double bonds. Scheme 4 also allows for the occurrence of a hydride shift which may be favored by the higher stability of allylic cations.

V. Mechanisms for the Formation of $C_6H_7^+$ and $C_9H_{12}^+$. Our postulated mechanism for the elimination of $C_6H_7^+$ in reaction 6 which competes with chain propagation is shown in Scheme 5. Here cyclization, elimination of protonated C_{60}, and a subsequent 1,2-H shift lead to the formation of protonated benzene, in a manner not unlike that observed for the reaction of allene radical cation with allene leading to H loss and the formation of $C_6H_7^+$.[33]

We suggest that the $m/z = 120$ cation, $C_9H_{12}^+$, produced in reactions 7 and 19 is the mesitylene (1,3,5-trimethylbenzene) cation or a closely related 1,2,3- or 1,2,4-trimethylbenzene isomer. These isomers are the most stable of the many isomers known for $C_9H_{12}^+$.[24] A plausible mechanism for the formation of the mesitylene cation which invokes the cylization of three allene units is shown in Scheme 6. Again it appears that cyclization is less favorable in the propyne derivative of C_{60}^{2+}, presumably due to charge delocalization. On the other hand, Coulomb repulsion in the triply-charged derivative appears to separate one of the charges sufficiently to overcome the barrier for mesitylene formation.

VI. Kinetics of Cation-Induced Polymerization. Table 1 summarizes the rate coefficients deduced by fitting the observed variations in ion signals to the solutions of the system of differential equations appropriate to the observed sequential reactions. For systems involving reaction steps with large variations in sequential rate coefficients, such as the reactions of $C_{60}(\text{allene})_n^{2+}$ with allene, the fitting procedure provides reliable rate coefficients only for the first few steps since solutions involve a sum of exponential terms. We note strong variations in the rate coefficients for the primary reactions, as well as for the higher-order addition reactions, with the charge on the C_{60}^{n+} cation for both the allene and propyne chemistry. The values of 3.1×10^{-11} and 1.6×10^{-10} cm^3 molecule^{-1} s^{-1} reported here for the addition of allene and propyne, respectively, to C_{60}^{2+} supersede the higher values of 8×10^{-11} and 5×10^{-10} cm^3 molecule^{-1} s^{-1} which we reported earlier.[35] The earlier values were obtained with an ion source with a different

(35) Petrie, S.; Javahery, G.; Wang, J.; Bohme, D. K. *J. Am. Chem. Soc.* **1992**, *114*, 9177.

Scheme 3

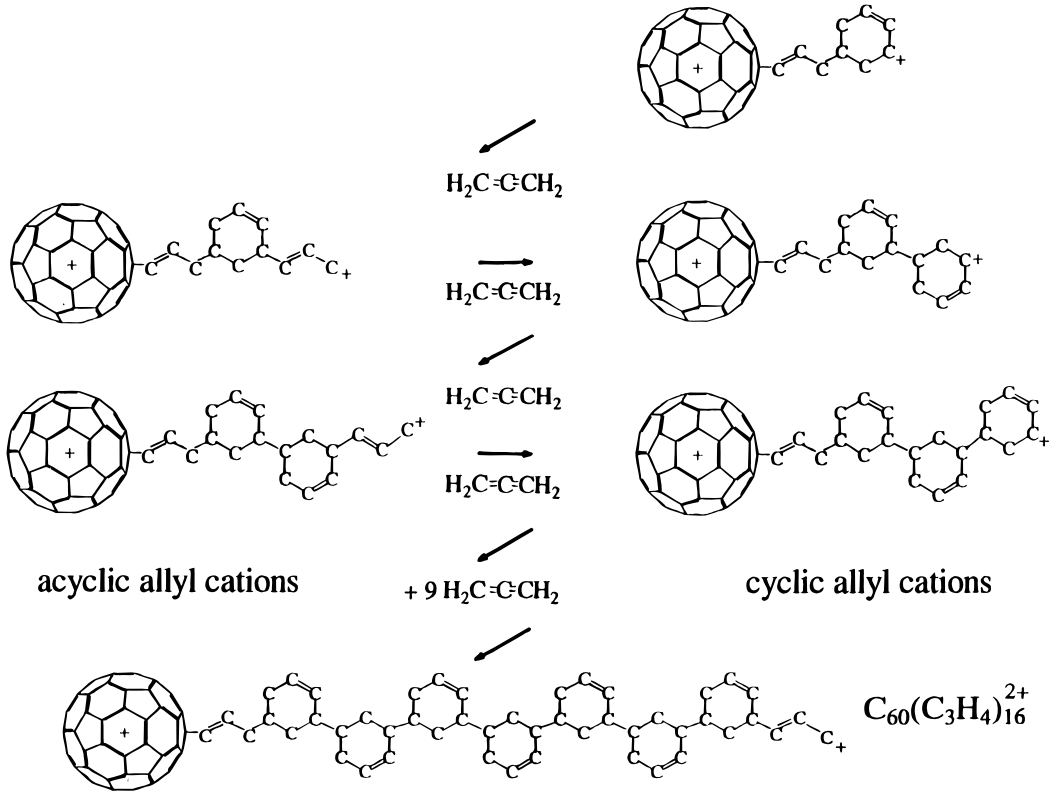

filament configuration and mode of heating the C_{60} which delivered much smaller (at least 20 times smaller) and less stable signals of C_{60}^{2+}. The observed decays in the C_{60}^{2+} were less than one order of magnitude and the accuracy associated with the rate coefficients determined from these decays was much less (an estimated accuracy of ±40% was reported).[35]

We attribute the failure to observe any addition of allene or propyne to C_{60}^{+} to the energy barrier associated with C−C bond formation which involves a rehybridization of the bonding C atom on C_{60} from largely sp^2 to sp^3.

Our results indicate that the first addition reactions of C_{60}^{2+} with allene and propyne proceed with an efficiency of approximately 1.6% and 7.0%, respectively, with the propyne reaction being more efficient. Here the efficiency is defined in the usual manner as the ratio of the measured reaction-rate coefficient to the calculated collision-rate coefficient, k_{obs}/k_{cap}, ×100%. The collison-rate coefficient, k_{cap}, is calculated using the ADO theory[36] but is only very approximate as it assumes that C_{60}^{2+} behaves as a point charge. The polarizabilities of allene and propyne were taken to be 5.92 and 6.18 Å^3, respectively, and their dipole moments 0 and 0.781 D,[37] respectively. Addition, accompanied by C−C bond formation with doubly-charged C_{60}^{2+}, is more probable than with C_{60}^{+} because of the stronger electrostatic attraction between reactants which may act to surmount the barrier associated with rehybridization.[38] The electrostatic attraction is stronger between C_{60}^{2+} and the more polar propyne molecule than between C_{60}^{2+}

Scheme 4

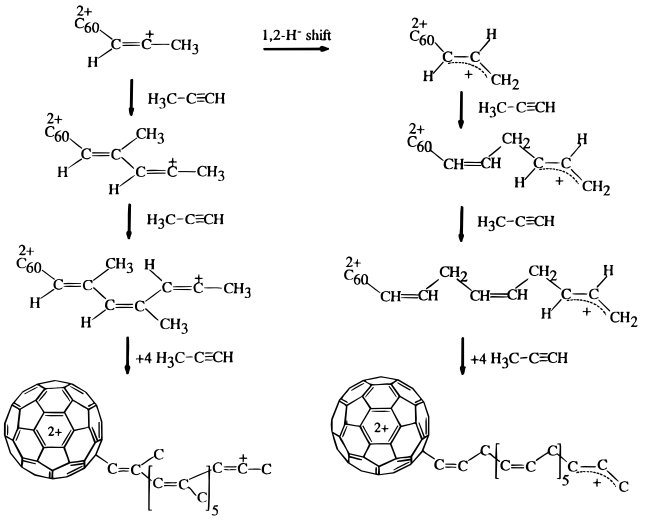

Scheme 5

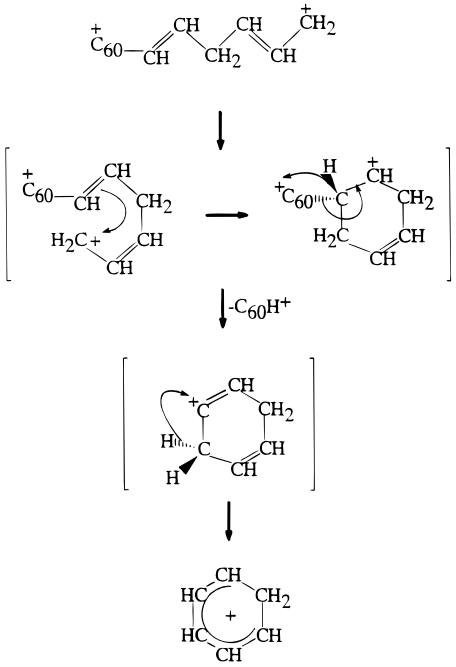

Scheme 6

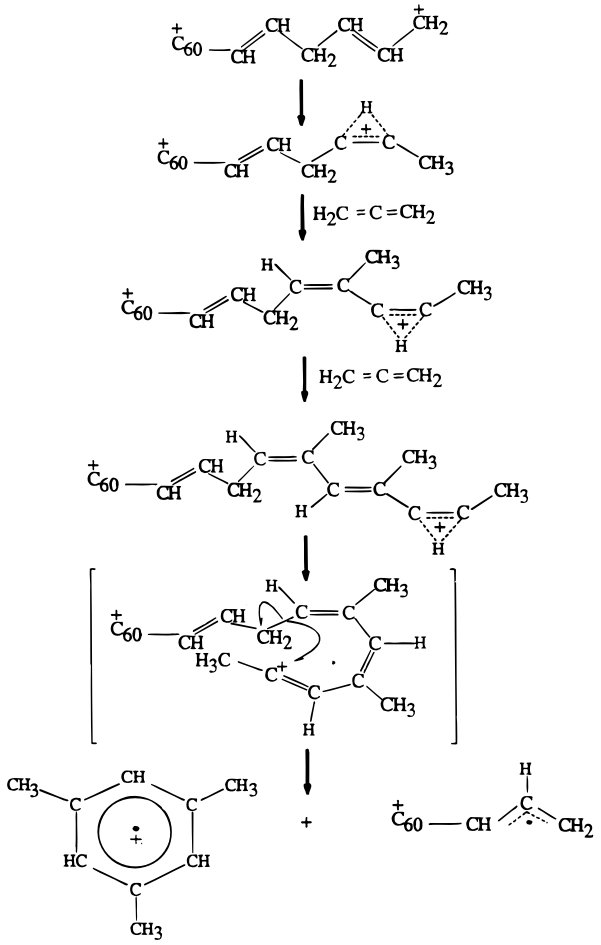

and allene and this may account for its higher reactivity relative to allene. The addition reaction between triply-charged C_{60}^{3+} and propyne proceeds much more rapidly, $k = 1.35 \times 10^{-9}$ cm^3 molecule^{-1} s^{-1}, and efficiently, efficiency = 39%, than either of the previous two addition reactions with C_{60}^{2+}. We attribute this higher reactivity to the stronger electrostatic attraction between reactants when the C_{60} is triply charged.[38]

The most remarkable feature in the observed higher-order reaction kinetics is the periodicity in the higher-order addition reactions of allene with $C_{60}(\text{allene})_n^{2+}$ with the even-numbered adducts reacting faster than the odd-numbered adduct ions. Although rate coefficients for the additions beyond 4 were not analyzed due to the increasing uncertainty associated with the fitting procedure, Figure 1 clearly shows that this alternating pattern in reactivity continues without any significant decrease in the relative reactivity of the even and odd adducts up to the addition of at least 12 molecules of allene. Indeed, we have observed this behavior to persist up to 16 additions of allene. On the basis of the relative magnitudes of the even-numbered and odd-numbered adduct ions, we estimate a factor of 10 difference in the relative rates of these reactions. In contrast, the addition reactions of propyne to $C_{60}(\text{propyne})_n^{2+}$ and $C_{60}(\text{propyne})_n^{3+}$ do not exhibit a periodic behavior in reaction kinetics up to 4 and 7 molecules, respectively. In our discussion of reaction mechanisms, we have accounted for this difference in kinetic behavior in terms of the occurrence of repeated cyclization and charge delocalization in the chain being propagated with allene. The allene adducts of C_{60}^{2+} with an even number of allene molecules are more charge localized and should react faster than those with an odd number of adducts in which the reacting charge is more delocalized owing to ring formation (except for the first adduct in which the charge is delocalized into the C_{60} cage). Also, the rate of formation of the latter charge-delocalized adducts is expected to be enhanced by their higher stability.

A general feature of the observed higher-order addition kinetics is a gradual decrease in the rate coefficient with the number of molecules added. Changes in the rate of chain propagation should be influenced in part by the availability and localization of the reactive charge at or near the end of the chain and in part by the stability of the new chain being formed. The dramatic difference in the extent of chain growth observed for allene and propyne, or difference in the rate with which the rate of chain propagation decreases with the number of monomers added, appears to be due primarily to the extra stability of the allene ball-and-chain as a consequence of cyclization. Also, since the Coulombic potential varies inversely with charge separation, the repulsion between the two positive charges will be relaxed as the carbon chain grows and this may lead to less charge localization and a lower rate of growth with increasing chain length. Moreover, chain growth should increase the flexibility of the chain and this may make the reactive charge site less accessible. However, the exact dynamics for chain growth remains uncertain and should provide a challenge for future analysis and calculation.

Conclusions

We have shown that dications and trications of C_{60} add allene and propyne sequentially at room temperature in a helium bath gas at 0.35 Torr, but that the monocation is unreactive. A remarkable alternation in reaction rate was observed for the multiple addition of allene to the dication (the trication reacts with allene only by electron transfer). Results of careful multi-collision induced dissociation experiments favor "ball-and-chain" structures for all of the adduct ions observed. Mechanisms have been proposed for the sequential addition reactions which, in the case of the sequential addition of allene to C_{60}^{2+}, lead to the formation of a chain of six-membered rings. Bimolecular reactions which were observed to compete with chain propagation have been attributed to the elimination of protonated benzene and the mesitylene cation.

Acknowledgment. D.K.B. is grateful to the Natural Sciences and Engineering Research Council of Canada for the financial support of this research.

JA961359J

(36) Su, T.; Bowers, M. T. *Int. J. Mass Spectom. Ion Phys.* **1973**, *12*, 347.

(37) *CRC Handbook of Chemistry and Physics*, 67th ed.; Weast, R. C., Ed.; CRC Press: Boca Raton, FL, 1986.

(38) Petrie, S.; Bohme, D. K. *Can. J. Chem.* **1994**, *72*, 577.